Fungal Genetics and Biology 154 (2021) 103598

Contents lists available at ScienceDirect

Fungal Genetics and Biology

journal homepage: www.elsevier.com/locate/yfgbi

Efficient genome editing using endogenous U6 snRNA promoter-driven CRISPR/Cas9 sgRNA in *Sclerotinia sclerotiorum*

Chenggang Wang, Jeffrey A. Rollins *

Department of Plant Pathology, 1450 Fifield Hall, University of Florida, Gainesville, FL, USA

ARTICLE INFO

Keywords:
CRISPR/Cas9
U6 promoter
Gene editing
S. sclerotiorum

ABSTRACT

We previously reported on a CRISPR-Cas9 genome editing system for the necrotrophic fungal plant pathogen *Sclerotinia sclerotiorum*. This system (the TrpC-sgRNA system), based on an RNA polymerase II (RNA Pol II) promoter (TrpC) to drive sgRNA transcription *in vivo*, was successful in creating gene insertion mutants. However, relatively low efficiency targeted gene editing hampered the application of this method for functional genomic research in *S. sclerotiorum*. To further optimize the CRISPR-Cas9 system, a plasmid-free Cas9 protein/sgRNA ribonucleoprotein (RNP)-mediated system (the RNP system) and a plasmid-based RNA polymerase III promoter (U6)-driven sgRNA transcription system (the U6-sgRNA system) were established and evaluated. The previously characterized oxaloacetate acetylhydrolase (*Ssoah1*) locus and a new locus encoding polyketide synthase12 (*Sspks12*) were targeted in this study to create loss-of-function mutants. The RNP system, similar to the TrpC-sgRNA system we previously reported, creates mutations at the *Ssoah1* gene locus with comparable efficiency. However, neither system successfully generated mutations at the *Sspks12* gene locus. The U6-sgRNA system exhibited a significantly higher efficiency of gene mutation at both loci. This technology provides a simple and efficient strategy for targeted gene mutation and thereby will accelerating the pace of research of pathogenicity and development in this economically important plant pathogen.

1. Introduction

S. sclerotiorum is one of the most devastating necrotrophic fungal plant pathogens in agriculture. It infects over 400 plant species and causes substantial yield losses in crops worldwide (Boland and Hall, 1994; Bolton et al., 2006). *S. sclerotiorum* has evolved several sophisticated virulence mechanisms to successfully attack its broad range of host plants. The ability to correctly sense, actively modulate, and dynamically respond to ambient pH has been demonstrated to be one of these key mechanisms (Kim et al., 2007; Liang et al., 2015; Rollins and Dickman, 2001; Xu et al., 2015). Additionally a number of putative effectors including the cerato-platanin protein SsCP1 and integrin-like protein SsITL have been shown to play important roles in virulence (Tang et al., 2020; Yang et al., 2018). From these studies, a two-phase infection model in which the pathogen first evades, counteracts and subverts host basal defense reactions prior to killing and degrading host cells has been proposed to understand the disease causing processes of *S. sclerotiorum* (Liang and Rollins, 2018). With genome-wide data available for *S. sclerotiorum*, developing an economical and efficient approach for gene mutation has become critical to determine gene function and better understand the molecular mechanism of pathogenesis.

Gene deletion by homologous recombination (Liang et al., 2015; Liberti et al., 2007; Rollins, 2003), gene transcript knockdown by RNA interference (RNAi) (Fan et al., 2017; Kim et al., 2011), random insertion mutations introduced by transfer DNA (T-DNA) (Xu and Chen, 2013; Xu et al., 2015), UV induced mutation (Godoy et al., 1990) and a TrpC promoter-driven CRISPR/Cas9 sgRNA system for targeted insertion mutagenesis (Li et al., 2018) have been developed to create gene mutations in *S. sclerotiorum*. However, these techniques are inefficient and time-consuming for screening large numbers of targeted gene mutations.

The CRISPR/Cas9 system, a key component of bacterial and archaeal adaptive immune systems (Horvath and Barrangou, 2010; Mojica et al., 2005; Wiedenheft et al., 2012), has been successfully developed as an efficient genome-editing tool in both prokaryotes and eukaryotes (Cong et al., 2013; Doudna and Charpentier, 2014; Sander and Joung, 2014; Shalem et al., 2015). The CRISPR-Cas9 system utilizes RNA-guided

* Corresponding author.
E-mail address: rollinsj@ufl.edu (J.A. Rollins).

https://doi.org/10.1016/j.fgb.2021.103598
Received 11 April 2021; Received in revised form 2 June 2021; Accepted 3 June 2021
Available online 10 June 2021

nuclease activity to introduce sequence-specific double-stranded breaks (DSBs) that can serve as targets for genome editing. As a tool, the system most commonly utilizes two components: a Cas9 endonuclease and an sgRNA; and two primary strategies to deliver the Cas9 endonuclease and the sgRNA into the cell: a plasmid-based system and a plasmid-free system (Nakamura et al., 2019; Wang, 2018). For the plasmid-free system, the purified Cas9 protein and transcribed sgRNAs can be assembled into a ribonucleoprotein (RNP) complex *in vitro* and delivered into competent cells to achieve cleavage of target sequences. Alternatively, a plasmid vector comprising a CAS9 protein expression cassette and an sgRNA expression cassette can be directly introduced into transformed cells transiently or stably by integration into the genome where the components are expressed and assembled. The establishment of CRISPR mutagenesis systems has been reported in plant pathogenic fungi and oomycetes including *Fusarium oxysporum* (Wang et al., 2018), *Magnaporthe oryzae* (Arazoe et al., 2015; Foster et al., 2018; Yamato et al., 2019), *Ustilago spp*. (Huck et al., 2019; Schuster, 2016), *Phytophthora* spp. (Fang and Tyler, 2016; Gumtow et al., 2018; Miao et al., 2018), *Botrytis cinerea* (Leisen et al., 2020), and *S. sclerotiorum* (Li et al., 2018). Efficiency of these systems varies and modification of the component parts has the potential to improve the targeting specificity and frequency of targeting events.

The sgRNA component of the CRISPR/Cas9 system contains a 20-nt RNA guide sequence complementary to the target DNA fused with the scaffold tracrRNA sequence (Mali et al., 2013). The sgRNA can recruit Cas9 to create a specific DNA double strand break (DSB) in the target sequence (Jinek et al., 2012). The DSB is generally repaired by error-prone non-homologous end-joining (NHEJ) leading to base-pair insertions or deletions (indels). The resulting frame shifts produce frequent loss-of-function mutations. DSBs may also be repaired by homologous recombination (HR) that is dependent on organism, locus, and cell cycle status (Lin et al., 2014). This offers another strategy to mediate precise genome editing when appropriate homologous donor DNA is present or provided and has been utilized in diverse organisms including fungi (Liu et al., 2015; Ran et al., 2013; Zou et al. 2020).

In *S. sclerotiorum*, a plasmid borne RNAP II promoter driven TrpC-sgRNA system (the TrpC-sgRNA system) has been demonstrated to create loss-of-function gene disruptions (Li et al., 2018). However, this procedure has not been widely adopted due to its relatively low efficiency in candidate target gene editing (Wang, Yu and Rollins, unpublished). We therefore set out to develop an optimized method to facilitate the applications of CRISPR/CAS9-based gene editing technology for efficiently creating gene specific mutations in this economically important pathogen. Delivery of purified Cas9 protein and *in vitro* synthesized sgRNA has also been demonstrated to effectively create gene-specific mutations in various fungal species (Al Abdallah et al., 2017; Grahl et al., 2017; Kuivanen and Richard, 2018; Min et al., 2016; Wang et al., 2018). Similar to plasmid-based delivery, the preassembled Cas9-sgRNA RNP complex can be delivered to fungal protoplasts by polyethylene glycol (PEG) or electroporation-mediated methods. These plasmid-free systems have the advantage of eliminating the possibility of foreign DNA integration. As an RNP-CRISPR system has not been reported for *S. sclerotiorum*, we also evaluated this strategy for efficient mutation of *S. sclerotium* genes.

In the plasmid-based CRISPR/Cas9 system, an efficient promoter to facilitate sgRNA transcription *in vivo* is a necessity (Ng and Dean, 2017; Song et al., 2018). The sgRNA in the CRISPR/Cas9 system does not require a cap structure or a polyA tail. In most CRISPR/Cas9 systems, sgRNA is driven by RNA polymerase type III U6 promoters that produce small, non-polyadenylated, nuclear RNAs. When RNA polymerase II (RNAP II) promoters, such as the strong PgpdA (Nødvig et al., 2015) or PmbfA promoters (Sarkari et al., 2017), are used, self-cleavage ribozymes, such as hepatitis delta virus (HDV) or Hammerhead (HH), are required at the 5′- and 3′-ends of the sgRNA (Gao and Zhao, 2014). Without these additions, the sgRNA conformation may be affected by reading-through of the transcript by RNA polymerase II (Nødvig et al., 2015). Never-the-less, the tryptophan C (TrpC) promoter (Yelton et al., 1984), an RNAP II promoter, has proven effective in driving sgRNA transcription at suitable levels for gene editing in *S. sclerotiorum* and in *P. oryzae* (Arazoe et al., 2015; Li et al., 2018). The U6 small nuclear RNA (snRNA) promoter, an RNA polymerase III (RNAP III) promoter, however, was shown to have higher gene editing efficiency than the TrpC promoter in *P. oryzae* (Arazoe et al., 2015; Carroll, 2014). Other U6 promoters have been used for efficient sgRNA transcription in filamentous fungi (Arazoe et al., 2015; Katayama et al., 2016; Liu et al., 2017; Pohl et al., 2016; Schuster et al., 2016; Zhang et al., 2016). A U6 promoter has not been identified and validated in *S. sclerotiorum* however. It is important to find reliable promoters to drive sgRNA transcription *in vivo* and to test their utility for efficient genome editing of *S. sclerotiorum*.

In this study, we aimed to establish a more efficient CRISPR/Cas9 system in *S. sclerotiorum*. Two strategies, a plasmid-free RNP and a plasmid-based delivery system were tested using *Ssoah1* and *Sspks12* gene loci as targets for mutation. Further, in the plasmid-based system, the RNAP III U6 and the RNAP II TrpC promoters were compared for efficacy of sgRNA production. Based on our results, the plasmid-based U6 promoter driven sgRNA system displays higher editing efficiency for candidate genes in *S. sclerotiorum*.

2. Materials and methods

2.1. Fungal strains, plants, and culture conditions

The *S. sclerotiorum* wild-type isolate UF1 (Li et al., 2018) was used to derive all strains in this study. Cultures were routinely grown on PDA (Difco, Detroit, MI, USA) at room temperature (22–24 °C). Transformants were cultured on PDA medium supplemented with 100 μg/mL hygromycin B (EMD Biosciences, La Jolla, CA, USA). Fungal stocks were stored on mycelium-colonized, desiccated filter paper or as dry sclerotia at −20 °C. The wild-type Arabidopsis (*Arabidopsis thaliana*) Columbia ecotype was utilized. The seeds were sown on autoclaved soil (Sunshine MVP; Sun Gro Horticulture) and cold treated at 4 °C for 3 d. Plants were germinated and grown at 23 °C to 25 °C under a 16-h-light/8-h-dark regime.

2.2. DNA constructs and genetic transformation

The endogenous *S. sclerotiorum* U6 promoter with sgRNA scaffold was synthesized and inserted between the NotI and XbaI sites of pCRISPR-Cas9-HYG-TrpC (Li et al., 2018), generating pCRISPR-Cas9-HYG-U6 (Fig. 2A). This vector has been made available to the scientific community through the Addgene plasmid depository (Addgene ID: 172069). Gene-specific sgRNA constructs were built by digesting these sgRNA expression plasmids with AarI and ligating double stranded oligonucleotides with the protospacer of the *Ssoah1* or *Sspks12* genes to yield pCRISPR-Cas9-HYG-U6 –*Ssoah1*sgRNA3, pCRISPR-Cas9-HYG-U6-*Sspks12*sgRNA1 and pCRISPR-Cas9-HYG-U6 - *Sspks12*sgRNA2. A detailed protocol for constructing gene-specific pCRISPR-Cas9-HYG-U6-sgRNA vectors is provided in Additional File 1. The donor DNA fragment HYG contained the TrpC promoter, open reading frame encoding hygromycin phosphotransferase (hph), and terminator was amplified from pCRISPR-Cas9-HYG-TrpC with Primers Hyg-PF and Hyg-TR. The donor DNA fragment 20 bp-HYG with micro-homologous arms was amplified from pCRISPR-Cas9-HYG-TrpC using the primers 20 bp-Hyg-FP and 20 bp-Hyg-TR containing 20-bp homologous arms, which were identical to the 5′ and 3′ flanking region of the *Ssoah1* sequence target site. After purification, approximately 6 μg of the PCR products of the donor DNA HYG or 20 bp-HYG were used directly for polyethylene glycol (PEG)-mediated genetic transformation of wild-type *S. sclerotiorum* protoplast following the methods of Rollins (2003). The same methods were followed for RNP transformations and selection on 100 μg/ml hygromycin B. Detailed descriptions of the sgRNA synthesis and RNP transformation are provided in Additional File 2.

2.3. Molecular analysis of transformants

Molecular detection of *Ssoah1* and *Sspks12* mutants was performed following six hyphal tip transfers of transformants on PDA medium supplemented with 100 ug/ml HygB. For primer-based confirmation of mutations, PCR was performed to amplify the *Ssoah1* fragment using *Ssoah1*-F and *Ssoah1*-R primers, the *Sspks12* fragment using PKS12F and PKS12R primers. Primers Hyg-C-F and Hyg-C-R were used to amplify of the hph coding sequence to characterize the hph gene insertion. Primers *Sspyc*-F and *Sspyc*-R designed to amplify *Sspyc*1 (GenBank accession no. XM_001586211) were used as a positive control to verify PCR amplification template quality.

Genomic DNA used as a template was isolated with the DNA mini-preparation protocol (Yelton et al., 1984). Taq DNA polymerase (New England BioLabs [NEB], Ipswich, MA) and LongAmp Taq DNA polymerase (NEB, Ipswich, MA) were used in combination with standard PCR components and standard programs used for PCR identification of the *Ssoah1* and *Sspks12* disruptions. All PCR primer sequences used in this study are given in Table S1 of the supplemental material.

2.4. CAS9 protein expression and purification

CAS9 protein expression and purification were performed as described by Wang et al. (2018) with minor modifications. Briefly, the *E. coli* Rosetta™(DE3) strain containing the plasmid pHis-parallel1-NLSH2BCas9 (Wang et al., 2018) was cultured at 37 °C in LB liquid medium with 100 μg/mL ampicillin to an OD600 of 0.6. IPTG was added to a final concentration of 0.3 mM and the culture incubated for an additional 16 h at 18 °C at 180 rpm on a rotary shaker. The culture was collected and suspended in 30 mL lysis buffer (20 mM NaH2PO4, 300 mM NaCl, 1 mM imidazole, 1% TritonX-100, 1 mM PMSF, pH 7.5) and lysed in an ultrasonic bath (15 s + 15 s, 10 min). The mixture was centrifuged and the supernatants were filtered with a 0.22 μm filter, and subsequent protein purification conducted using HisPur™ Ni-NTA Chromatography Cartridges (Thermo Fisher Scientific). The eluted Cas9 protein was further dialyzed against the Cas9 buffer (20 mM NaH2PO4, 300 mM NaCl, 10% glycerol, pH 7.5) for 6–8 h. The dialyzed Cas9 protein was centrifuged and the associated un-dissolved protein was removed. The Cas9 protein was further concentrated with a 100 K centrifugal filter to a final concentration of 4 mg/mL.

2.5. In vitro Cas9 nuclease cleavage assay

The Cas9 nuclease cleavage assay *in vitro* was conducted in a system with 20 μL total volume (1 μL diluted purified Cas9 protein, 40 ng sgRNA, 1 × Cas9 Nuclease Reaction Buffer, 3 μL 20 nM PCR fragment, DEPC-treated water). All items were added together and incubated 37 °C for 1 h. The final products were analyzed on a 0.8% agarose gel.

2.6. Compound appressorium assay

Fresh mycelial plugs (5-mm diameter) with growing hyphal tips were placed on paraffin film (Parafilm M; Bemis NA, Neenah, WI) and incubated in a humidity chamber for 3 days. Compound appressoria could be observed macroscopically by the presence of pigmented development surrounding the agar plug. Compound appressoria for macroscopic observations were also produced on GelAir cellophane (Bio-Rad, Hercules, CA). For this, four agar plugs from PDA cultures were placed onto PDA plates overlaid with cellophane and incubated for 3 days.

2.7. Pathogenicity assays

Freshly collected 4-week-old Arabidopsis leaves were inoculated with agar plugs taken from the edge of 1- to 2-day-old *S. sclerotiorum* cultures on PDA and incubated at room temperature. Eight leaves were inoculated with each strain. The experiment was repeated three times. Timing and symptom development were recorded.

2.8. Radial growth and sclerotial development

Colony radial growth was investigated in the wild-type and knockout strains. A 5-mm mycelial plug from the edge of an actively growing colony was excised and transferred to a fresh PDA plate (90 mm). The wild-type, empty vector control strain and four *Sspks12* gene knockout strains were assayed with three replicates. At 1-day intervals in a 24-day time course, the hyphal growth and sclerotial development of the wild-type and knockout strains were recorded.

3. Results

3.1. Gene disruption of the Ssoah1 gene using the RNP system

We previously reported the introduction of large sequence insertions at targeted locations in the *Ssoah1* and *SsPKS13* gene loci through a plasmid-based CRISPR/CAS9 system in *S. sclerotiorum* (Li et al., 2018). To determine whether a plasmid-free RNP system also has utility for gene editing in *S. sclerotiorum*, the *Ssoah1* gene locus was again targeted. This locus was chosen based on its ease of phenotypic screening. As SsOah1 catalyzes oxalic acid synthesis by hydrolyzing oxaloacetate (Liang et al., 2015; Maxwell, 1973), successful *Ssoah1* gene mutation can be assessed with medium acidification assays. Wild type and non-mutant transformants change the color of the pH-indicating medium from blue to yellow as oxalic acid accumulates while loss-of-function *Ssoah1* mutants remain blue. Thus, preliminary mutagenic targeting efficiency could be easily discerned from the ratios of blue and yellow colonies.

The Cas9 protein with a nuclear localization sequence was expressed and purified as described by Wang et al. (2018) with minor modifications detailed in the Materials and Methods (Supplemental Fig. S1A). Validated target site number 3 of the *Ssoah1* gene (Li et al., 2018) was selected as the target and sgRNA (*Ssoah1*sgRNA-3) synthesized. A Cas9 *in vitro* nuclease cleavage assay was conducted to evaluate the efficiency of target site cleavage. A 690 bp PCR fragment containing the coding region of the *Ssoah1* gene was mixed with *Ssoah1*sgRNA-3 and the Cas9 protein. The Cas9-*Ssoah1*sgRNA3 complex was able to cleave nearly all of the template *in vitro* within an hour and the fragments were of the expected size. (Supplemental Fig. S1B).

In *S. sclerotiorum*, 1–2 kb of homologous sequences upstream and downstream of the donor DNA sequence can mediate HR for gene replacements (Rollins, 2003). Low HR efficiency and donor DNA construction steps are disadvantages to using HR as a gene disruption or deletion tool. Recent reports suggest that micro-homology sequences are sufficient to precisely insert novel DNA sequences at CRISPR/CAS9-induced DSBs by short donor DNAs with high efficiency in some fungi (Nødvig et al., 2018; Pohl et al., 2016; Zhang et al., 2016). In order to increase the frequency of HR and simplify the construction of donor DNA in pCRISPR/CAS9 system, we tested whether short 20 bp homologous arms that are easily added to the ends of the donor DNA through direct primer synthesis, can induce DSB repair via the HR repair pathway in *S. sclerotiorum*. An amplified donor DNA fragment containing 20 bp of sequence identical to the flanking sequences on either side of the target cleavage site were added to each end of a 1,778 bp hygromycin phosphotransferase gene cassette (20 bp-HYG) and used as a dominant selection marker and donor DNA fragment in transformations.

To quantify relative gene editing efficiency with the plasmid-free RNP system, the plasmid-based (pCRISPR-CAS9-TrpC) RNAP II TrpC-sgRNA system (Arazoe et al., 2015; Li et al., 2018) was employed as a control (Fig. 1A). Both the plasmid-based pCRISPR-CAS9-TrpC-*Ssoah1sg*RNA3 and the *in vitro* preassembled CAS9/*Ssoah1*-sgRNA3s complex, were separately mixed with donor DNA fragments: the hygromycin phosphotransferase gene cassette (HYG) or the HYG with 20 bp of homologous sequence up-stream and down-stream of the

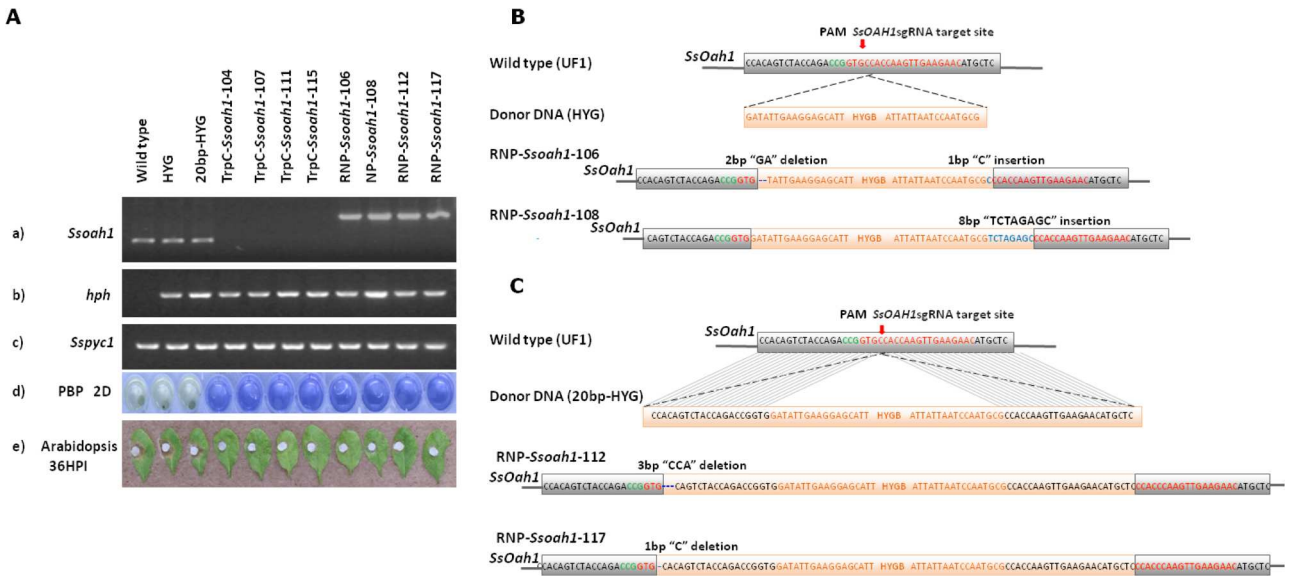

Fig. 1. PCR screening of the *Ssoah1* gene disruptants and DNA sequence of the resulting amplicons. (A) (a) Long-amplification PCR of *Ssoah1* mutants (TrpC-Ssoah1-###) with primer *Ssoah1*-F and *Ssoah1*-R. (b) Long-amplification PCR with primer pair Hyg-C-F and Hyg-C-R. (c) Primers *Sspyc*-F and *Sspyc*-R specific to the *Sspyc1* gene (XM_001586211) were used as a positive PCR control. Primer sequences are given in Table S. (d) Colony morphology on PDA amended with bromophenol blue (PBP). Photographs were taken at four days (4d) after inoculation. (e) Virulence assays on detached Arabidopsis leaves. Photographs were taken at 36 h post-inoculation (HPI). (B) Amplicon sequencing showing the integration of donor DNA HYG through error-prone NHEJ (non-homologous end joining). The PAM sequence is highlighted in green, whereas the sgRNA guiding sequence is highlighted in red. Nucleotide deletions and substitutions are depicted in blue. (C) Amplicon sequencing showing the integration of donor DNA 20 bp-HYG through error-prone NHEJ. The PAM sequence is highlighted in green, whereas the sgRNA guiding sequence is highlighted in red. Nucleotide deletions and substitutions are depicted in blue. (For interpretation of the references to color in this figure legend, the reader is referred to the web version of this article.)

Ssoah1 target site attached to the 5′ and 3′ ends of the HYG cassette (20 bp-HYG). These mixtures were delivered into protoplast cells via PEG–mediated transformation. Following genetic transformation and six rounds of hyphal tip purification on hygromycin selection medium, transformants were screened on potato dextrose agar (PDA) supplemented with the pH indicator dye bromophenol blue (BPB). Results of the screen indicate the RNP systems, similar to TrpC-sgRNA system, can effectively edit the *Ssoah1* gene to generate *Ssoah1* mutants with comparable efficiency (Table 1). The DNA plasmid lacking sgRNA and the donor DNA fragment alone failed to produce transformants with the mutant phenotype (Table 1).

Ssoah1 gene disruption was molecularly confirmed through a PCR screen. Ten phenotypically identified mutants created with the plasmid-based TrpC-sgRNA system or the plasmid-free RNP system were randomly selected and analyzed by PCR amplification. In the plasmid-based TrpC-sgRNA system, all of the examined phenotypic mutants including those with HYG or 20 bp-HYG donor DNA, consistent with our previous reports, failed to amplify across the target sequence due to large sequence insertions at the target site and showed a severely attenuated virulence on Arabidopsis (Fig. S2A, Fig. 1A). In the RNP system, all of the examined phenotypic mutants, including those with HYG or 20 bp-HYG donor DNA, successfully amplified a 2.4 kb DNA bands across the target sequence and exhibited severely attenuated virulence on Arabidopsis (Fig. S2B, Fig. 1A). These results indicated that a donor DNA insertion event occurred in the target gene sequence with both methods. To further validate that mutations in the RNP transformants were caused by DNA cleavage and foreign DNA insertion at the target site, the PCR products of the *Ssoah1* gene amplifications were sequenced in 4 phenotypic mutants generated from donor DNA HYG or 20 bp-HYG. All the selected *Ssoah1* mutants displayed an insertion of the donor DNA fragment at the expected target site located 3 bp upstream of the Protospacer Adjacent Motif (PAM) sequence (Fig. 1B). Furthermore, these sequenced donor DNA insertion positions, including those from HYG or 20 bp-HYG, contained small nucleotide insertions or deletions ranging in size from a single nucleotide to 8 bp (Fig. 1B). Sequencing results show that these donor DNA insertions are derived from a NHEJ-mediated DSB repair pathway. No HR-mediated repair events were obtained indicating that a 20 bp homologous arms were not sufficient for HR mediated repair of CRISPR/Cas9 induced DSB in *S. sclerotiorum*.

3.2. The U6 promoter driven sgRNA plasmid promotes high efficiency Ssoah1 gene mutation

To explore the utility of the endogenous *S. sclerotiorum* U6 promoter to drive sgRNA transcription in the plasmid-based pCRISPR/CAS9 system, we queried the *S. sclerotiorum* genome for the highly conserved U6 snRNA gene (GenBank accession:MW302327). The putative promoter region encompassing 700 bp upstream of the gene was used as the endogenous U6 promoter for these studies. The TrpC promoter in our backbone vector pCRISPR-Cas9-HYG-TrpC (Arazoe et al., 2015; Li et al., 2018) was replaced with this endogenous U6 promoter to create vector pCRISPR-Cas9-HYG-U6 (Fig. 2A). To compare the relative effectiveness of the U6 promoter and the TrpC promoter, both CRISPR/Cas9 expression vectors were used to target the *Ssoah1* gene locus.

pCRISPR-Cas9-HYG-U6-*Ssoah1*sgRNA3 and pCRISPR-Cas9-HYG-TrpC-*Ssoah1*sgRNA3 vectors, were delivered into protoplast cells via PEG-mediated transformation. The blue-yellow phenotypic screen showed that the frequency of mutant phenotypes obtained with the endogenous U6 driven-*Ssoah1*sgRNA3 vector was greater than twice that of the TrpC-sgRNA system (Table 2). Control transformations with the backbone vector controls: pCRISPR-Cas9-HYG-U6 and pCRISPR-Cas9-HYG-TrpC lacking sgRNA sequences did not produce mutants (Table 2). These results demonstrate that the promoter used to transcribe sgRNA has a great influence in RNA-guided nuclease activities with the U6 promoter driven sgRNA exhibiting a higher mutation frequency at the *Ssoah1* locus.

Nine phenotypically identified mutants created from each plasmid-based sgRNA transcription system were randomly selected and analyzed by PCR amplification. Transformants obtained from the TrpC-sgRNA system, consistent with our previous reports, failed to amplify

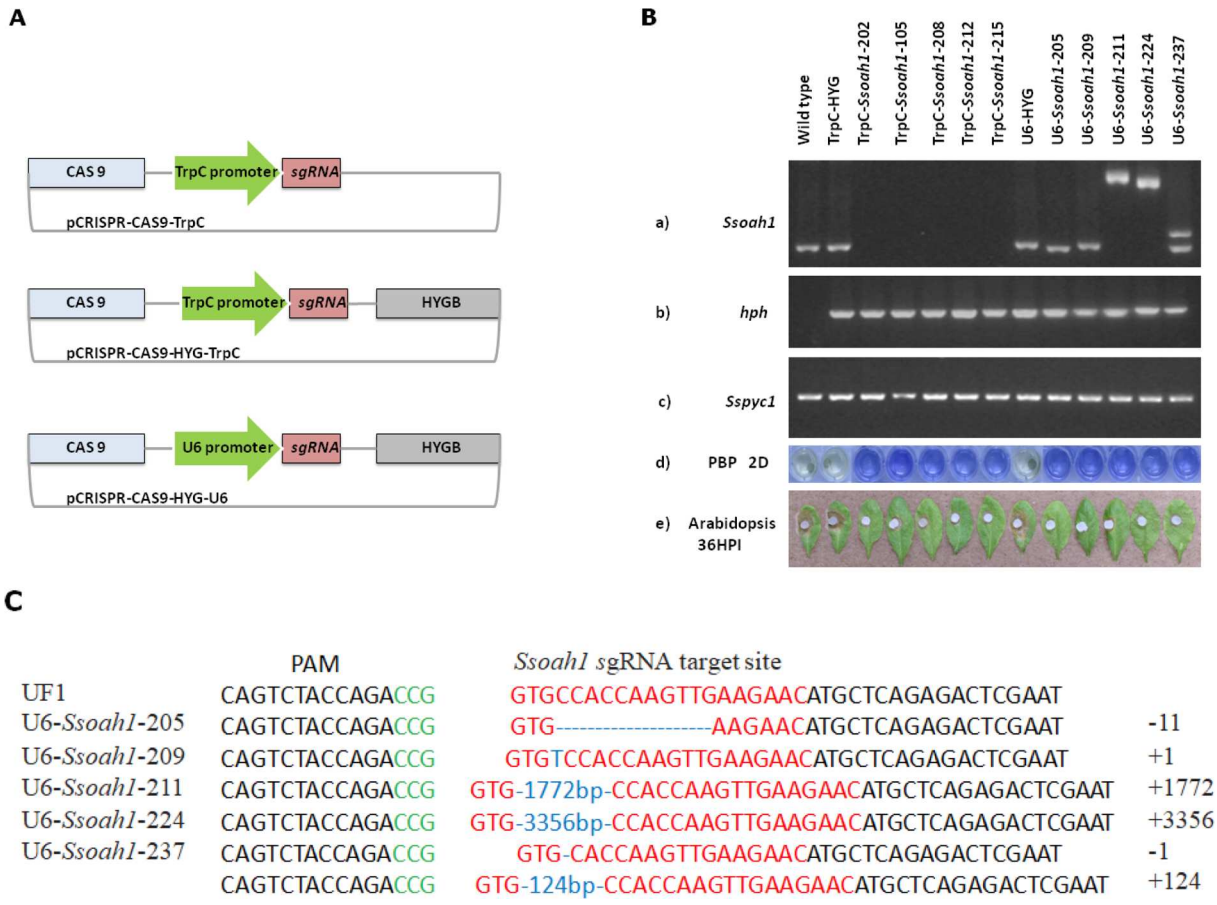

Fig. 2. PCR screening of *Ssoah1* gene disruptants. (A) Schematic illustration of three pCRISPR/Cas9-expressing plasmids. (B) (a) Long-amplification PCR of *Ssoah1* mutants (TrpC-Ssoah1-### and U6-Ssoah1-###) with primer *Ssoah1*-F and *Ssoah1*-R. (b) Long-amplification PCR with primer pair Hyg-C-F and Hyg-C-R. (c) Primers *Sspyc*-F and *Sspyc*-R specific to the *Sspyc1* gene (XM_001586211) were used as a positive PCR control. Primer sequences are given in Table S1. (d) Colony morphology on PDA amended with bromophenol blue (PBP). Photographs were taken at four days (4d) after inoculation. (e) Virulence assays on detached Arabidopsis leaves. Photographs were taken at 36 h post-inoculation (HPI). (C) Sequence alignments of the *Ssoah1* locus from wild type (UF1) and five independent transformants. The PAM sequence is highlighted in green, whereas the sgRNA sequence is highlighted in red. Nucleotide deletions and substitutions are depicted in blue. (For interpretation of the references to color in this figure legend, the reader is referred to the web version of this article.)

Table 1
Gene editing efficiency of TrpC-sgRNA/RNP systems in the *Ssoah1* locus.

Transgene	Total	*Ssoah1* mutant	Efficiency
pCRISPR-Cas9-TrpC-*Ssoah1*sgRNA3	0	0	0%
HYG	3	0	0%
20 bp-HYG	4	0	0%
pCRISPR-Cas9-TrpC-*Ssoah1*sgRNA3 + HYG	39	13	33.3%
pCRISPR-Cas9-TrpC-*Ssoah1*sgRNA3 + 20 bp-HYG	37	12	32.4%
RNP (Cas9 + *Ssoah1*sgRNA3) + HYG	26	9	34.6%
RNP (Cas9 + *Ssoah1*sgRNA3) + 20 bp-HYG	31	11	35.5%

Table 2
Gene editing efficiency of TrpC promoter and U6 promoter in the *Ssoah1* locus.

Transgene	Total	*Ssoah1* mutant	Efficiency
pCRISPR-Cas9-HYG-TrpC	11	0	0%
pCRIPSR-Cas9-HYG-TrpC-*Ssoah1*sgRNA3	42	15	35.7%
pCRISPR-Cas9-HYG-U6	14	0	0%
pCRISPR-Cas9-HYG-U6 -*Ssoah1*sgRNA3	74	64	86.5%

across the target sequence due to large sequence insertions at the target site (Fig. S3A). These transformants exhibited severely attenuated virulence on Arabidopsis (Fig. 2B). With the U6-sgRNA system, most (eight of nine) of the examined phenotypic mutants successfully amplified across the target site (Fig. 2B, Fig. S3B). Subsequent amplicon sequencing from five of these randomly selected mutants was performed. The length of indels ranged in size from 1 bp to 4 kb at the targeted cleavage site of these *Ssoah1* mutants, consistent with the fact that CRISPR/Cas9-guided DSBs can be repaired through the error-prone NHEJ mechanism. Compared with the TrpC-sgRNA system, the NHEJ-mediated DSB repair in the U6-sgRNA system displays a high frequency of small insertions and deletions (indels), and the integration of foreign plasmid DNA into the DSB site is rare.

3.3. The U6 promoter driven sgRNA plasmid promotes high efficiency *Sspks12* gene mutation

To further investigate whether the U6-sgRNA system is applicable to other genomic loci in *S. sclerotiorum*, the *Sspks12* gene predicted to encode a polyketide synthase for melanin biosynthesis (GenBank accession:XM_001586710), was targeted. Two sgRNAs (*Sspks12*sgRNA1 and *Sspks12*sgRNA2) located within the starter unit acyl carrier protein transacylase (SAT) and beta-ketoacyl synthase (KS) -encoding domains of SsPks12 were designed to evaluate RNA-guided nucleases activity with the U6-sgRNA system (Fig. 3A).

Four pCRISPR/Cas9 vectors expressing two *Sspks12* sgRNAs driven by the U6 or TrpC promoter were constructed and delivered into protoplasts via PEG-mediated transformation. The *Bcpks12* deletion mutant

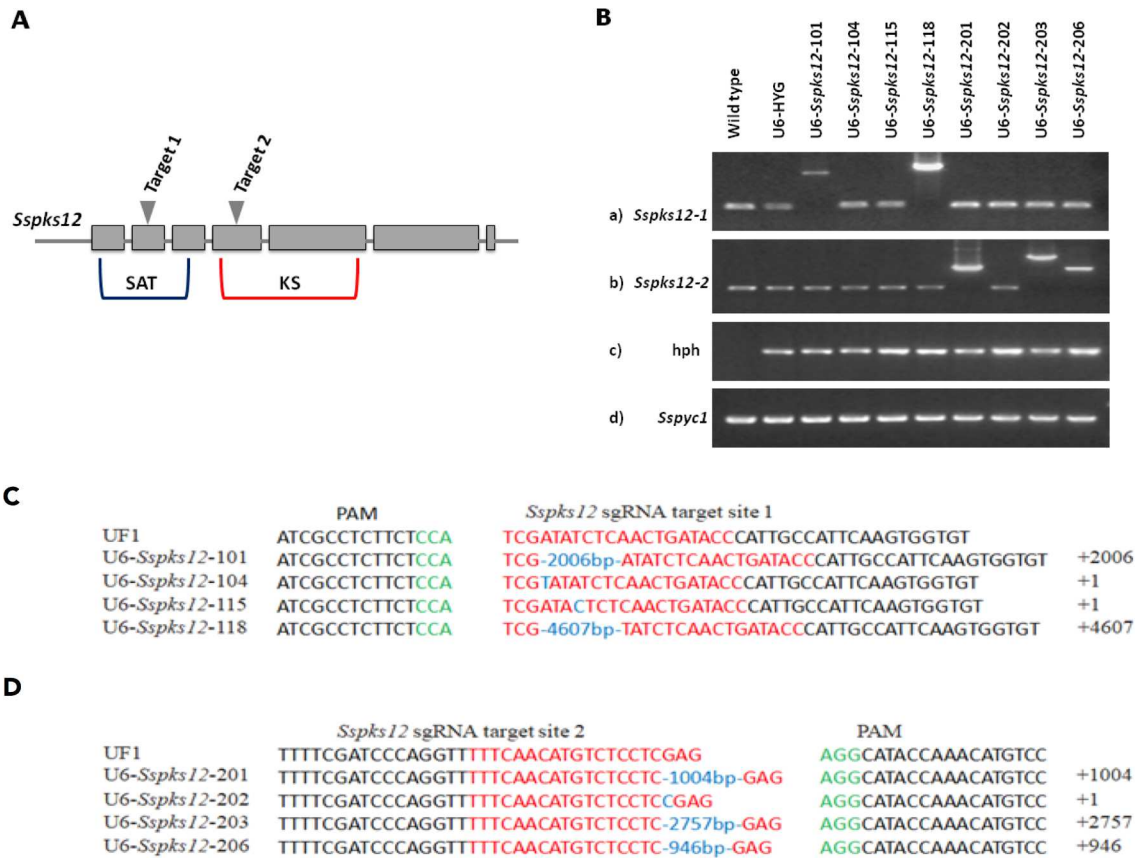

Fig. 3. Creation of CRISPR-Cas9-derived *Sspks12* mutants. (A) Cas9 target site locations within the encoded domains of SsPKS12. Starter unit acyl carrier protein transacylase (SAT); beta-ketoacyl synthase domain (KS). (B) (a) Long-amplification PCR of wild type, empty vector control transformants (U6-HYG) and *Sspks12* mutants (U6-Sspks12-###) with primer pair *Sspks12-1*-F and *Sspks12-1*-R (for *Sspks12* target 1 locus) or *Sspks12-2*-F and *Sspks12-2*-R (for *Sspks12* target 2 locus). (b) Long-amplification PCR with primer pair Hyg-C-F and Hyg-C-R. (c) Primers *Sspyc*-F and *Sspyc*-R specific to the *Sspyc1* gene (XM_001586211) were used as a positive PCR control. Primer sequences are given in Table S1. (C) DNA sequence alignment of the *Sspks12* target 1 locus of wild type (UF1) and four mutants. The PAM sequence is highlighted in green, whereas the sgRNA sequence is highlighted in red. Nucleotide deletions and substitutions are depicted in blue. (D) DNA sequence alignment of the *Sspks12* target 2 locus of wild type (UF1) and four mutants. The PAM sequence is highlighted in green, whereas the sgRNA sequence is highlighted in red. Nucleotide deletions and substitutions are depicted in blue. (For interpretation of the references to color in this figure legend, the reader is referred to the web version of this article.)

in *Botrytis cinerea* produces white to yellowish sclerotia (Schumacher, 2016). During the initial selection of *Sspks12* transformants, some transformants were found to produce light brown sclerotia (Fig. 4A). PCR analysis and DNA sequencing confirmed that these light brown sclerotia-producing transformants were *Sspks12* mutants (Fig. 3B, C and D). The production of light brown sclerotia became an important basis for our subsequent rapid screening and identification of *Sspks12* mutants. *Sspks12* mutants were obtained only from the U6-sgRNA plasmid system (Table 3). No *Sspks12* mutants were obtained from the TrpC-sgRNA plasmid system for either *Sspks12* target sites or with the pCRISPR/Cas9-backbone vector controls (Table 3).

Two different *Sspks12* sgRNA target sites (*Sspks12*sgRNA1 and *Sspks12*sgRNA2) show comparable gene mutation efficiency in the U6-sgRNA system (Table 3). Nine transformants were randomly selected for PCR analysis of the *Sspks12* target sites. Variable sized DNA bands were successfully amplified across the target sequence of most of the examined mutants, only a few mutants failed to amplify across the target sequence indicating a large DNA insertion event at the target site (Fig. S4A, S4B, Fig. 3B). Eight sequenced *Sspks12* mutants from two different *Sspks12* sgRNA target sites displayed a range of insertions close to the PAM site (Fig. 3C, 3D).

The RNP system was also tested for *Sspks12* gene mutation, however no transformants displaying the mutant phenotype were obtained (data not shown). These studies show that among the systems tested here, the U6-sgRNA system has the highest success rate for CRISPR-Cas9-based candidate target gene mutation in *S. sclerotiorum*.

3.4. Phenotypic characterization of Sspks12 mutants

As gene mutations in the *Sspks12* gene have not been previously reported, we phenotypically characterized these mutants. The radial growth of the wild-type and the *Sspks12* mutant strains on potato dextrose agar (PDA) plates was investigated with a time course study. Compared to wild type and control transformants, *Sspks12* disruption did not affect mycelial growth, the initiation and development of sclerotia, or the number and size of sclerotia (Fig. 4A). However, the pigmentation of sclerotia was reduced in *Sspks12* mutants with the sclerotia exhibiting a light brown color (Fig. 4A). Following conditioning and incubation for carpogenic germination, sclerotia of the *Sspks12* mutants germinated to produce albino apothecia (Fig. 4B). *Sspks13*, another polyketide synthase encoding gene involved in melanin biosynthesis was previously determined to be involved in pigmentation of compound appressoria in *S. sclerotiorum* (Li et al., 2018). To investigate whether *Sspks12* disruption affected compound appressorium development and pigmentation, fresh mycelial plugs of four *Sspks12* mutants, wild-type and control transformants were incubated on paraffin film and on cellophane for 3 days. All *Sspks12* mutants produce compound appressoria with wild-type pigmentation and development (Fig. 4C). The virulence of the *Sspks12* mutants were assessed on Arabidopsis. The size of the lesions produced by the *Sspks12* disruption

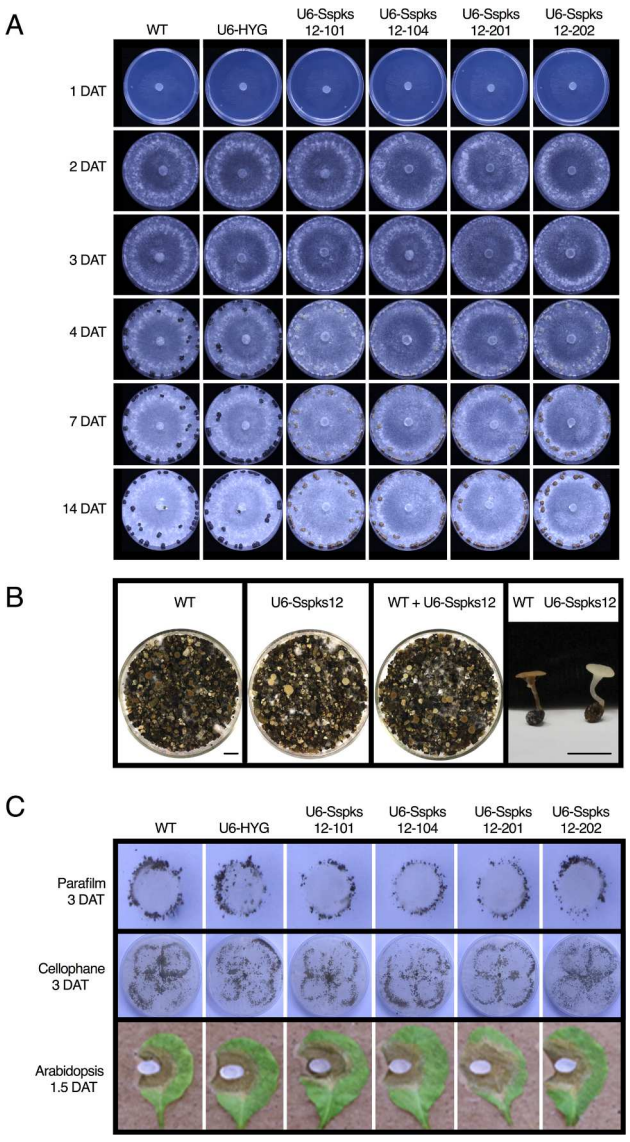

Fig. 4. Phenotypic characterization of *Sspks12* mutants. (A) Vegetative hyphae growth and development of sclerotia of the wild type (WT), control transformant (U6-HYG) and the *Sspks12* gene knockout mutants U6-*Sspks12*-101/104/201/202 over time. (DAT: days after transfer). (B) Apothecia of wild type (WT) and the *Sspks12* gene knockout mutant U6-*Sspks12*-101. Apothecia produced from sclerotia incubated in moist vermiculate are shown for the wild type (WT), the *Sspks12* gene knockout mutant U6-*Sspks12*-101, and a mixture of WT and U6-*Sspks12*-101 sclerotia to provide contrast. (C) Compound appressorium development and virulence assays of the wild type (WT), control transformant (U6-HYG) and individual *Sspks12* gene knockout mutants. Hyphae colonized PDA agar plugs were placed on paraffin film, cellophane, and detached Arabidopsis leaves and pictures taken at the indicated days after transfer (DAT). The dark pigmentation on the paraffin film and cellophane is indicative of pigmented compound appressorium development.

Table 3
Gene editing efficiency of TrpC promoter and U6 promoter in the *Sspks12* locus.

Transgene	Total	*Sspks12* mutant	Efficiency
pCrispr-Cas9-HYG-TrpC	11	0	0%
pCrispr-Cas9-HYG-TrpC-Sspks12sgRNA1	37	0	0%
pCrispr-Cas9-HYG-TrpC-*Sspks12*sgRNA2	36	0	0%
pCrispr-Cas9-HYG-U6	14	0	0%
pCrispr-Cas9-HYG-U6-*Sspks12*sgRNA1	49	35	71.4%
pCrispr-Cas9-HYG-U6-*Sspks12*sgRNA2	51	39	76.4%

mutants were indistinguishable from that of the wild type and control transformants (Fig. 4C). These observations demonstrate that *Sspks12* mutants form normal compound appressoria in size and pigmentation, normal sclerotia in size and numbers but lacking black pigmentation, and that sclerotia are competent for carpogenic germination giving rise to albino apothecia.

4. Discussion

In this work, we compared two different methods, a plasmid-free RNP system and a plasmid-based system to create CRISPR-Cas9-based gene-specific mutations in *S. sclerotiorum*. The plasmid-free RNP system has been widely used in different organisms such as mouse, human, grape, apple, tobacco, and fungi (Kim et al., 2014; Malnoy et al., 2016; Min et al., 2016; Wang et al., 2018; Woo et al., 2015). Plasmid-based systems have also been used in a range of organisms including fungi (Arazoe et al., 2015; Long et al., 2018; Song et al., 2018; Tsutsui and Higashiyama, 2017; Zheng et al., 2018). We targeted two genes based on the ease of phenotyping loss-of-function mutations: the previously characterized *Ssoah1* gene required for oxalic acid biosynthesis and the previously uncharacterized *Sspks12* gene that we determined here is required for pigment accumulation in sclerotia and apothecia.

Our findings show that the RNP system can effectively introduce gene mutations at the *Ssoah1* locus but when we attempted to employ this system to target the *Sspks12* gene with two different sgRNAs, no *Sspks12* mutants were obtained. This finding indicates that the success rate for candidate target gene editing is limited when our RNP system is employed in *S. sclerotiorum*. Considering the high cost of *in vitro* CAS9 protein purification and sgRNA synthesis, this technique may be useful when mutations or gene edits without generating transgenics is an important consideration.

For the plasmid-based system, we further tested the gene mutation frequency of sgRNA transcription driven by two different promoters: the RNA Pol II-dependent TrpC promoter derived from *Aspergillus nidulans* (Yelton et al., 1984) and the RNA Pol III-dependent endogenous U6 promoter from *S. sclerotiorum*. The plasmid-based TrpC-sgRNA system mutated the *Ssoah1* locus but at relatively low frequency and, as with the RNP-system, failed to generate mutatioins at the *Sspks12* locus. In contrast, the plasmid-based U6-sgRNA system created gene mutations at both the *Ssoah1* and the *Sspks12* locus with relatively high frequency. The presence of sufficient numbers of functioning CAS9/sgRNA complexes *in vivo* may be an important limiting factor for gene targeting in *S. sclerotiorum*. Introduction of these components via RNP complexes is finite compared to the plasmid-based sgRNA transcription system with potentially continuous and stable expression of CAS9 and sgRNA. This may explain the low efficiency of the RNP-system. Differences in the efficiency and frequency of mutant recovery in the plasmid-based system is likely due to differences in sgRNA production by the two promoters. An efficient promoter can drive sgRNA transcription to form sgRNA molecules but differences in RNA polymerases driving transcription from a given promoter will dictate the formation of stable, mature sgRNA molecules in the optimal subcellular location to form a complex with the Cas9 protein. The results demonstrate that sgRNA transcription generated from both the U6 and the TrpC promoter could facilitate the necessary DSB for NHEJ-mediated events at the *Ssoah1* locus, but, the sgRNA driven by the U6 promoter resulted in significantly higher mutation frequency than that driven by the TrpC promoter. Furthermore, at the *Sspks12* locus, the U6 promoter-driven sgRNA provided high gene mutation frequency whereas no gene mutations were obtained from TrpC-sgRNA system. Presumably, the TrpC promoter does not contain self-splicing ribozyme sequences flanking the sgRNA sequence, which obstruct the mature sgRNA transcript (Nødvig et al., 2015). Additionally polyadenylated sgRNAs derived from the Trpc RNA Pol II promoter would be exported to the cytoplasm after processing where they associate with the Cas9 protein before reentering the nucleus. Presumably both factors contribute to the lower efficiency of

utilizing the TrpC promoter to drive transcription of stable and mature sgRNA transcripts. Another significant difference between the use of TrpC and U6 promoters to drive the expression of sgRNA was the rate of exogenous DNA incorporation within the DSB target site. One hundred percent of the TrpC-sgRNA transformants incorporated large inserts of exogenous (plasmid) DNA at the target site. This is consistent with our previous findings with this construct at the *Ssoah1* and the *Sspks13* loci (Li et al., 2018). In contrast, only one third of the U6-sgRNA transformants incorporated exogenous (plasmid) DNA into the DSB target sites. In addition, with the U6-sgRNA system, NHEJ-mediated DSB-repair introduced more diverse indels, and more fragmented plasmid DNA integration, compare with predominantly large vector DNA insertion events found in the TrpC promoter-driven sgRNA system. Although we hypothesize that high concentrations of plasmid DNA exist in the nuclei of *S. sclerotiorum* during transformation and differences in the efficiency of DNA cleavage and repair are responsible for these findings, the mechanism behind these differences is currently unknown.

In this work we also evaluated the utility of providing our selectable marker gene cassette with short DNA sequences identical to the genomic sequences flanking the CRISPR/Cas9 target site to determine if the DSB produced by CRISP-Cas9 would facilitate homologous recombination (HR) with short regions of homologous sequences. HR is an important pathway for the repair of double-stranded DNA breaks in fungi and gene targeting by homologous recombination is a powerful tool to precisely manipulate the genome for genetic engineering (Klein, 1995; Rudin and Haber, 1988). HR frequency in somatic cells however, is very low (<5%) in filamentous fungi (Fuller et al., 2015; Meyer et al., 2007). In traditional gene editing methods, efficiency is typically improved by increasing the length of homologous arms. For example, the gene deletion efficiency was enhanced from 4 to 29%, when the homologous arm was increased from 100 bp to 1500 bp (Meyer et al., 2007). The shortened donor DNA homologous arms were reported to improve the HR frequency to repair double-stranded DNA breaks caused by Cas9 in *T. reesei* (Liu et al., 2015), *A. fumigates* (Zhang et al., 2016) and *P. chrysogenum* (Pohl et al., 2016). In our work we utilized donor DNA with 20 bp homologous arms to test HR events in the RNP system at the *Ssoah1* locus. Transformants with integrated donor DNA at the target site were recovered at a reasonable frequency. Our sequencing results revealed, however, that with 20 bp homologous arms, donor DNAs was still inserted into the DSB site through the NHEJ pathway. Constructing longer homology arms that can mediate HR to repair CAS9/sgRNA-induced DSBs may increase efficiency but come at the expense of increased costs and time to prepare constructs. Further experimentation is required to determine the shortest length of homology required for the donor DNA to facilitate HR at DSB-sites in *S. sclerotiorum*. Together HR and pCRISPR/Cas9-mediated DSBs may provide precision guidance for performing sequence manipulations that the pCRISPR/Cas9 system alone cannot deliver. For simple introduction of random mutations at a specific genomic sequence, however, the pCRISPR/Cas9 system utilizing the RNAP III U6 promoter (U6-sgRNA system) is efficient and cost effective.

The development of the U6-sgRNA CRISPR-Cas9 system allowed us to explore new aspects of *S. sclerotiorum* biology in this study. Two polyketide synthase (PKS) genes are encoded in the *S. sclerotiorum* genome orthologous to the PKS genes previously demonstrated in *B. cinerea* to be required for development-specific 1,8-dihydroxynaphthalene (DHN) -melanin accumulation (Schumacher, 2016). The first of these PKSs, Pks13, was previously reported in *S. sclerotiorum* to be responsible for melanin accumulation in compound appressoria (Li et al., 2018). The ortholog in *B. cinerea* (*Bcpks13*) was demonstrated to be required for melanin accumulation in conidia (Schumacher, 2016). In the current work we created a loss of function mutant in the *Sspks12* gene. The orthologous gene in *B. cinerea* (*Bcpks12*) is responsible for melanin accumulation in *B. cinerea* sclerotia (Schumacher, 2016). Interestingly, in both *B. cinerea* and *S. sclerotiorum*, although the sclerotium rind no longer accumulates melanin, sclerotia still retain light pigment accumulation which can vary depending on growth media (Schumacher, 2016). We further demonstrate here for *S. sclerotiorum* that the sclerotia of the *Sspks12* mutant are competent for carpogenic germination and that the resulting apothecia are albino rather than their usual buff color. Further biochemical characterization of the accumulating pigments in both wild type and the loss-of-function mutants should provide a better understanding of the relationships between DHN melanin biosynthesis, precursor or shunt metabolite accumulation, DHN crosslinking and other pigment accumulation as they relate to development and functions in sclerotia and apothecia of Sclerotiniacea species.

In summary, comparison of RNP-, TrpC- and U6-based CRISPR-Cas9 systems for introduction of coding sequence mutations at two independent loci determined that all exhibited gene-specific targeting but that the U6 system was the most efficient. The adaptability, efficiency and specificity of this tool allow us now to explore the pathogenesis and developmental biology of *S. sclerotiorum* at a genome-wide level.

CRediT authorship contribution statement

Chenggang Wang: Conceptualization, Investigation, Methodology, Validation, Writing - original draft. **Jeffrey A. Rollins:** Conceptualization, Validation, Supervision, Writing - review & editing, Funding acquisition.

Declaration of Competing Interest

The authors declare that they have no known competing financial interests or personal relationships that could have appeared to influence the work reported in this paper.

Acknowledgments

We gratefully acknowledge Takayuki Arazoe at Meiji University for providing the initial CRISPR-Cas9-TrpC vector, Jeffrey J. Coleman at Auburn University for providing the plasmid pHis-parallel1-NLSH2BCas9, and Zhonglin Mou at the University of Florida for providing the Arabidopsis col-0 seeds. Funding for this research was provided by National Science Foundation Award ID 1758932 and the ARS National Sclerotinia Initiative Cooperative Agreement #58-3060-6-033.

Appendix A. Supplementary material

Supplementary data to this article can be found online at https://doi.org/10.1016/j.fgb.2021.103598.

References

Al Abdallah, Q., et al., 2017. A simple and universal system for gene manipulation in *Aspergillus fumigatus*: in vitro-assembled Cas9-guide RNA ribonucleoproteins coupled with microhomology repair templates. Msphere. 2.
Arazoe, T., et al., 2015. Tailor-made CRISPR/Cas system for highly efficient targeted gene replacement in the rice blast fungus. Biotechnol. Bioeng. 112, 2543–2549.
Boland, G., Hall, R., 1994. Index of plant hosts of *Sclerotinia sclerotiorum*. Can. J. Plant Pathol. 16, 93–108.
Bolton, M.D., et al., 2006. *Sclerotinia sclerotiorum* (Lib.) de Bary: biology and molecular traits of a cosmopolitan pathogen. Molecular Plant Patholol. 7, 1–16.
Carroll, D., 2014. Genome engineering with targetable nucleases. Annu. Rev. Biochem. 83, 409–439.
Cong, L., et al., 2013. Multiplex genome engineering using CRISPR/Cas systems. Science 339, 819–823.
Doudna, J.A., Charpentier, E., 2014. The new frontier of genome engineering with CRISPR-Cas9. Science 346.
Fan, H., et al., 2017. An atypical forkhead-containing transcription factor SsFKH1 is involved in sclerotial formation and is essential for pathogenicity in *Sclerotinia sclerotiorum*. Mol. Plant Pathol. 18, 963–975.
Fang, Y., Tyler, B.M., 2016. Efficient disruption and replacement of an effector gene in the oomycete P hytophthora sojae using CRISPR/C as9. Mol. Plant Pathol. 17, 127–139.

Foster, A.J., et al., 2018. CRISPR-Cas9 ribonucleoprotein-mediated co-editing and counterselection in the rice blast fungus. Sci. Rep. 8, 1–12.
Fuller, K.K., et al., 2015. Development of the CRISPR/Cas9 system for targeted gene disruption in *Aspergillus fumigatus*. Eukaryot. Cell 14, 1073–1080.
Gao, Y., Zhao, Y., 2014. Self-processing of ribozyme-flanked RNAs into guide RNAs in vitro and in vivo for CRISPR-mediated genome editing. J. Integr. Plant Biol. 56, 343–349.
Godoy, G., et al., 1990. Use of mutants to demonstrate the role of oxalic acid in pathogenicity of *Sclerotinia sclerotiorum* on Phaseolus vulgaris. Physiol. Mol. Plant Pathol. 37, 179–191.
Grahl, N., et al., 2017. Use of RNA-protein complexes for genome editing in non-albicans *Candida* species. Msphere. 2.
Gumtow, R., et al., 2018. A *Phytophthora palmivora* extracellular cystatin-like protease inhibitor targets papain to contribute to virulence on papaya. Mol. Plant Microbe Interact. 31, 363–373.
Horvath, P., Barrangou, R., 2010. CRISPR/Cas, the immune system of bacteria and archaea. Science 327, 167–170.
Huck, S., et al., 2019. Marker-free genome editing in Ustilago trichophora with the CRISPR-Cas9 technology. RNA Biol. 16, 397–403.
Jinek, M., et al., 2012. A programmable dual-RNA–guided DNA endonuclease in adaptive bacterial immunity. Science 337, 816–821.
Katayama, T., et al., 2016. Development of a genome editing technique using the CRISPR/Cas9 system in the industrial filamentous fungus *Aspergillus oryzae*. Biotechnol. Lett. 38, 637–642.
Kim, H.-J., et al., 2011. Identification and characterization of *Sclerotinia sclerotiorum* NADPH oxidases. Appl. Environ. Microbiol. 77, 7721–7729.
Kim, S., et al., 2014. Highly efficient RNA-guided genome editing in human cells via delivery of purified Cas9 ribonucleoproteins. Genome Res. 24, 1012–1019.
Kim, Y.T., et al., 2007. An activating mutation of the *Sclerotinia sclerotiorum pac1* gene increases oxalic acid production at low pH but decreases virulence. Mol. Plant Pathol. 8, 611–622.
Klein, H.L., 1995. Genetic control of intrachromosomal recombination. BioEssays 17, 147–159.
Kuivanen, J., Richard, P., 2018. NADPH-dependent 5-keto-D-gluconate reductase is a part of the fungal pathway for D-glucuronate catabolism. FEBS Lett. 592, 71–77.
Leisen, T., et al., 2020. CRISPR/Cas with ribonucleoprotein complexes and transiently selected telomere vectors allows highly efficient marker-free and multiple genome editing in *Botrytis cinerea*. PLoS Pathog. 16, e1008326.
Li, J., et al., 2018. Introduction of large sequence inserts by CRISPR-Cas9 to create pathogenicity mutants in the multinucleate filamentous pathogen *Sclerotinia sclerotiorum*. MBio. 9.
Liang, X., et al., 2015. Oxaloacetate acetylhydrolase gene mutants of *Sclerotinia sclerotiorum* do not accumulate oxalic acid, but do produce limited lesions on host plants. Mol. Plant Pathol. 16, 559–571.
Liang, X., Rollins, J.A., 2018. Mechanisms of broad host range necrotrophic pathogenesis in *Sclerotinia sclerotiorum*. Phytopathology 108, 1128–1140.
Liberti, D., Grant, S.J., Benny, U., Rollins, J.A., Dobinson, K.F., 2007. Development of an *Agrobacterium tumefaciens*-mediated gene disruption method for *Sclerotinia sclerotiorum*. Can. J. Plant Pathol. 29, 394–400.
Lin, S., Staahl, B.T., Alla, R.K., Doudna, J.A., 2014. Enhanced homology-directed human genome engineering by controlled timing of CRISPR/Cas9 delivery. eLife 3, e04766.
Liu, Q., et al., 2017. Development of a genome-editing CRISPR/Cas9 system in thermophilic fungal Myceliophthora species and its application to hyper-cellulase production strain engineering. Biotechnol. Biofuels 10, 1–14.
Liu, R., et al., 2015. Efficient genome editing in filamentous fungus *Trichoderma reesei* using the CRISPR/Cas9 system. Cell Discovery 1, 1–11.
Long, L., et al., 2018. Optimization of CRISPR/Cas9 genome editing in cotton by improved sgRNA expression. Plant Methods 14, 85.
Mali, P., et al., 2013. RNA-guided human genome engineering via Cas9. Science 339, 823–826.
Malnoy, M., et al., 2016. DNA-free genetically edited grapevine and apple protoplast using CRISPR/Cas9 ribonucleoproteins. Front. Plant Sci. 7, 1904.
Maxwell, D.P., 1973. Oxalate formation in *Whetzelinia sclerotiorum* by oxaloacetate acetylhydrolase. Physiol. Plant Pathol. 3, 279–288.
Meyer, V., et al., 2007. Highly efficient gene targeting in the *Aspergillus niger* kusA mutant. J. Biotechnol. 128, 770–775.
Miao, J., et al., 2018. Mutations in ORP1 conferring oxathiapiprolin resistance confirmed by genome editing using CRISPR/Cas9 in *Phytophthora capsici* and *P. sojae*. Phytopathology. 108, 1412–1419.
Min, K., et al., 2016. *Candida albicans* gene deletion with a transient CRISPR-Cas9 system. Msphere. 1.
Mojica, F.J.M., Díez-Villaseñor, C., García-Martínez, J., Soria, E., 2005. Intervening sequences of regularly spaced prokaryotic repeats derive from foreign genetic elements. J. Mol. Evol. 60, 174–182.
Nakamura, M., et al., 2019. Plasmid-based and-free methods using CRISPR/Cas9 system for replacement of targeted genes in *Colletotrichum sansevieriae*. Sci. Rep. 9, 1–10.
Ng, H., Dean, N., 2017. Dramatic improvement of CRISPR/Cas9 editing in *Candida albicans* by increased single guide RNA expression. Msphere. 2.
Nødvig, C.S., et al., 2018. Efficient oligo nucleotide mediated CRISPR-Cas9 gene editing in Aspergilli. Fungal Genet. Biol. 115, 78–89.
Nødvig, C.S., et al., 2015. A CRISPR-Cas9 system for genetic engineering of filamentous fungi. PLoS ONE 10, e0133085.
Pohl, C., et al., 2016. CRISPR/Cas9 based genome editing of *Penicillium chrysogenum*. ACS Synth. Biol. 5, 754–764.
Ran, F.A., et al., 2013. Genome engineering using the CRISPR-Cas9 system. Nat. Protoc. 8, 2281–2308.
Rollins, J.A., 2003. The *Sclerotinia sclerotiorum pac1* gene is required for sclerotial development and virulence. Mol. Plant Microbe Interact. 16, 785–795.
Rollins, J.A., Dickman, M.B., 2001. pH signaling in *Sclerotinia sclerotiorum*: identification of a pacC/RIM1 homolog. Appl. Environ. Microbiol. 67, 75–81.
Rudin, N., Haber, J., 1988. Efficient repair of HO-induced chromosomal breaks in *Saccharomyces cerevisiae* by recombination between flanking homologous sequences. Mol. Cell. Biol. 8, 3918–3928.
Sander, J.D., Joung, J.K., 2014. CRISPR-Cas systems for editing, regulating and targeting genomes. Nat. Biotechnol. 32, 347–355.
Sarkari, P., et al., 2017. An efficient tool for metabolic pathway construction and gene integration for *Aspergillus niger*. Bioresour. Technol. 245, 1327–1333.
Schumacher, J., 2016. DHN melanin biosynthesis in the plant pathogenic fungus *Botrytis cinerea* is based on two developmentally regulated key enzyme (PKS)-encoding genes. Mol. Microbiol. 99, 729–748.
Schuster, M., et al., 2016. Genome editing in *Ustilago maydis* using the CRISPR–Cas system. Fungal Genet. Biol. 89, 3–9.
Shalem, O., et al., 2015. High-throughput functional genomics using CRISPR–Cas9. Nat. Rev. Genet. 16, 299–311.
Song, L., et al., 2018. Efficient genome editing using tRNA promoter-driven CRISPR/Cas9 gRNA in *Aspergillus niger*. PLoS ONE 13, e0202868.
Tang, L., et al., 2020. An effector of a necrotrophic fungal pathogen targets the calcium-sensing receptor in chloroplasts to inhibit host resistance. Mol. Plant Pathol 21, 686–701.
Tsutsui, H., Higashiyama, T., 2017. pKAMA-ITACHI vectors for highly efficient CRISPR/Cas9-mediated gene knockout in *Arabidopsis thaliana*. Plant Cell Physiol. 58, 46–56.
Wang, P., 2018. Two distinct approaches for CRISPR-Cas9-mediated gene editing in *Cryptococcus neoformans* and related species. Msphere. 3, e00208–18.
Wang, Q., et al., 2018. Efficient genome editing in *Fusarium oxysporum* based on CRISPR/Cas9 ribonucleoprotein complexes. Fungal Genet. Biol. 117, 21–29.
Wiedenheft, B., et al., 2012. RNA-guided genetic silencing systems in bacteria and archaea. Nature 482, 331–338.
Woo, J.W., et al., 2015. DNA-free genome editing in plants with preassembled CRISPR-Cas9 ribonucleoproteins. Nat. Biotechnol. 33, 1162–1164.
Xu, L., Chen, W., 2013. Random T-DNA mutagenesis identifies a Cu/Zn superoxide dismutase gene as a virulence factor of *Sclerotinia sclerotiorum*. Mol. Plant Microbe Interact. 26, 431–441.
Xu, L., et al., 2015. pH dependency of sclerotial development and pathogenicity revealed by using genetically defined oxalate-minus mutants of *Sclerotinia sclerotiorum*. Environ. Microbiol. 17, 2896–2909.
Yamato, T., et al., 2019. Single crossover-mediated targeted nucleotide substitution and knock-in strategies with CRISPR/Cas9 system in the rice blast fungus. Sci. Rep. 9, 1–8.
Yang, G., et al., 2018. A cerato-platanin protein SsCP1 targets plant PR1 and contributes to virulence of *Sclerotinia sclerotiorum*. New Phytol. 217, 739–755.
Yelton, M.M., et al., 1984. Transformation of *Aspergillus nidulans* by using a trpC plasmid. Proc. Natl. Acad. Sci. 81, 1470–1474.
Zhang, C., et al., 2016. Highly efficient CRISPR mutagenesis by microhomology-mediated end joining in *Aspergillus fumigatus*. Fungal Genet. Biol. 86, 47–57.
Zheng, X., et al., 2018. Heterologous and endogenous U6 snRNA promoters enable CRISPR/Cas9 mediated genome editing in *Aspergillus niger*. Fungal Biol. Biotechnol. 5, 2.
Zou, G., Xiao, M., Chai, S., Zhu, Z., Wang, Y., Zhou, Z., 2020. Efficient genome editing in filamentous fungi via an improved CRISPR-Cas9 ribonucleoprotein method facilitated by chemical reagents. Microb. Biotechnol. https://doi.org/10.1111/1751-7915.13652.